

Behavior of a Large Diameter Piles Subjected to Moment and Lateral Loads

Vijayakanthan KUNASEGARAM

PhD Student, Dept. of Civil and Environmental Engineering, Tokyo Institute of Technology, Tokyo, Japan

Email: vijayakanthan.k.aa@m.titech.ac.jp, heshuvijay@gmail.com

Wei Hsuan HSIAO

Master's Student, Dept. of Civil and Environmental Engineering, Tokyo Institute of Technology, Tokyo, Japan

Sakae SEKI

Technician, Dept. of Civil and Environmental Engineering, Tokyo Institute of Technology, Tokyo, Japan

Jiro TAKEMURA

Associate Professor, Dept. of Civil and Environmental Engineering, Tokyo Institute of Technology, Tokyo, Japan

ABSTRACT

This paper discusses the influence of embedment depth and embedded medium on the behaviour of laterally loaded large diameter steel tubular piles with relatively large moment loads based on centrifuge model tests under cyclic lateral loading. Embedded media tested were Toyoura sands with 80% and 95% relative densities, and a soft sand rock. From the loading tests, two failure modes of the pile foundation were observed, i.e., ground failure and pile structural failure depending on the embedment depth and ground strength. Due to the large moment load and rigidity in the embedded portion, the latter failure mode tends to dominate in hard mediums. For the pile with relatively small embedment depth, the increase of embedment depth can increase the lateral and moment resistance. However, as the embedment depth increases, the effect of the depth becomes less significant, especially for ultimate resistance due to the pile structural failure. "Optimum embedment depths" over which the increase of horizontal resistance becomes less are, depending on the initial lateral stiffness and ultimate bearing capacity, shallower for that of the stiffness than the ultimate bearing capacity. From the abovementioned observations, it was confirmed that the determination of the rational embedment depth considering given conditions is the most critical step in the design of this type of pile foundation.

Key words: *Large diameter piles, Embedment depth, Soft rock, Dense sand, Centrifuge model, Cyclic lateral loads*

1. Introduction

Wind turbines are one of the promising sustainable energy sources in the 21st century. Among various types of foundations, mono-pile foundation, namely a large diameter pile, is a desirable option for a wind turbine due to its simplicity in construction. Thanks to high structural stiffness and strength, large diameter steel tubular piles can be applied for various large geotechnical structures, such as a mono-pile foundation and a large height self-standing retaining wall. A typical loading condition to the mono-pile foundation is relatively large moment loads due to high elevation of lateral loading from the turbine. However, the behaviour of large diameter piles subjected

to massive moment loads has not been well understood due to the difficulties of conducting large scale tests to observe the behaviour of piles, which are controlled by several influential factors, such as pile factors (diameter, stiffness, embedment depth), ground factors (strength and stiffness), and loading factors (loading height, monotonic and cyclic). On the other hand, conventional design methods based on p-y curves often yield a large installation depth with a high margin of safety, which might not be an economical solution for the large diameter piles. Therefore, the development of a rational design method for the very stiff large diameter pile foundation is required, in which several factors and potential critical

behaviours are taken into account. For the application of these structures with rational embedment depths, the stability against the imposed lateral and large moment loads must be secured by the resistance from the embedded medium.

This paper reports the behavior of single steel tubular piles subjected to lateral and moment loads, based on 50g centrifuge model tests. Influences of embedment depths, embedded mediums and the loading history on the behavior of single piles embedded in stiff grounds were investigated.

2. Centrifuge models and test procedures

Three different ground conditions were made in the centrifuge models, such as medium dense sand, dense sand and soft sand rock. Setups of centrifuge model tests for piles embedded in Toyoura sand with two different relative densities (80% & 95%), and soft rock are shown in **Fig. 1** and **Fig. 2** respectively. Detailed mechanical properties of Toyoura sand were reported by Tatsuoka et al. (1986) including the effects of density, and the mechanical properties of model soft rock used was described in Kunasegaram et al. (2015).

Different containers were used for the sand models and the rock model, with the internal dimensions of 802mm length, 400mm depth and 250mm width, and 700mm length, 500mm depth and 150mm width respectively. Model tubular piles used in this study were thin wall pipes with 40mm outer diameter and 0.5mm thickness, made of stainless steel (SUS304) having the young's modulus (E) of 193 GPa and yield stress (σ_y) of 255 MPa. At the pile top, aluminum made solid circular pile cap with 30mm socked depth was tightly fixed to form a solid loading head. Sectional and mechanical properties of steel tubular piles are described in **Table. 1**. The model piles were equipped with bending strain gauges on both sides of the pile along the loading direction and Wheatstone circuits were made with the help of bridge boxes. Up on completion of the bridge arrangement, test piles were calibrated with known weights and a lever arm so that the piles could experience the stresses below the yield strain. Once the calibration completed, the strain gauges were coated with a thin film of epoxy resin in order to prevent the damaging of strain gauges under high compressive stresses at 50g centrifugal acceleration.

Bending strains were measured by using full bridge circuits along the pile, while at the pile tip a pair of half bridge circuits were utilized to measure the axial strains at the loading side and the opposite side independently. For the sand model, model grounds with 390 mm thickness were made using Toyoura sand with relative densities of 80% (Model-1) and 95% (Model-2) by air-pluviation as shown in **Fig. 1**. Upon completion of the model ground with desired densities, three model piles with different embedment depths ($d_e=130\text{mm}$, Pile-S; 180mm, Pile-M; 230mm, Pile-L) were installed vertically in the model ground with the help of pile guide. The section and mechanical properties of piles which were used in Model-1 and Model-2 are identical.

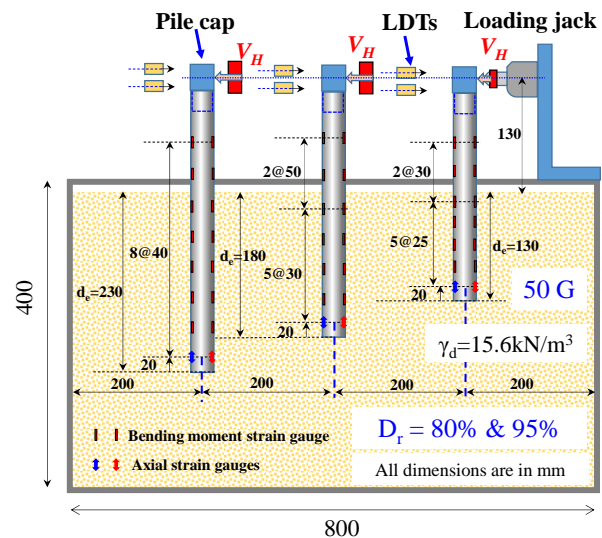


Fig. 1 Experiment set up for piles embedded in Toyoura sand Model-1 and Model -2

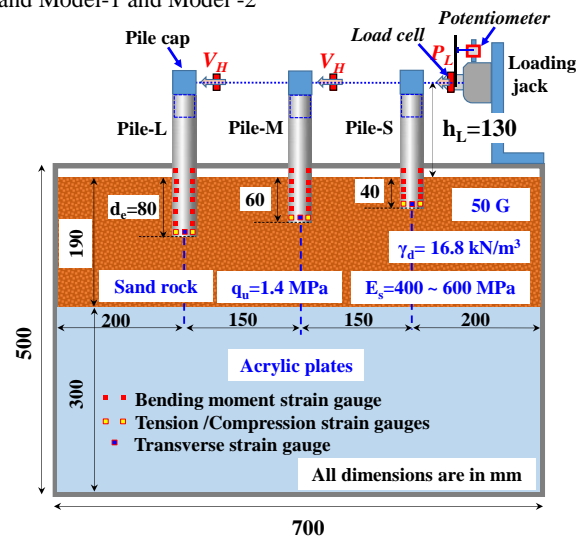


Fig. 2 Experiment set up for piles embedded in soft rock Model-3

Table 1. Experiment conditions and properties of steel tubular pile (Model scales are given in parenthesis)

Embedded medium	Properties of embedded medium	Pile Notation	Embedment depth (m)	Loading height (m)	Pile dimensions	EI (GNm ² /m) M _y & M _p (MNm)
Model-1 Toyoura sand Dr=80% (MS)	$\gamma_d=15.5 \text{ kN/m}^3$ $\phi'=40^\circ$	MS_S	6.5 (130 mm)	6.5 (130mm)	$\Phi=2 \text{ m}$ $t = 25 \text{ mm}$ $\left(\begin{array}{l} \Phi=40 \text{ mm} \\ t=0.5 \text{ mm} \end{array} \right)$	EI=14.6 (2.34×10^{-6}) M _y =19.3 (0.154×10^{-3}) M _p =24.8 (0.198×10^{-3})
		MS_M	9 (180 mm)			
		MS_L	11.5 (230 mm)			
Model-2 Toyoura sand Dr=95%	$\gamma_d=16.0 \text{ kN/m}^3$ $\phi'=43^\circ$	DS_S	6.5 (130 mm)			
		DS_M	9 (180 mm)			
		DS_L	11.5 (230 mm)			
Model-3 Soft sand rock (SR)	$\gamma_d=16.8 \text{ kN/m}^3$ $q_u=1.3\text{-}1.4 \text{ MPa}$ $E_s=400\text{-}600 \text{ MPa}$	SR_S*	2 (40 mm)			
		SR_M	3 (60 mm)			
		SR_L	4 (80 mm)			

EI: Pile flexural rigidity, M_y: Bend moment causing pile yielding, M_p: bending moment causing pile plastic failure,

ϕ' : friction angle from Triaxial compression with $\sigma_3'=98 \text{ kPa}$ (Tatsuoka et al, 1986), *Preloaded prior to the test without instrumentation

Centrifuge model arrangement for three single piles embedded ($d_e=40 \text{ mm}$, Pile-S; 60 mm , Pile-M; 80 mm , Pile-L) in soft sand rock is described in **Fig. 2**. In the preparation of soft rock model, 300 mm thick acrylic plates stack was tightly placed in the container bottom to reduce the depth to 200 mm . A 190 mm thick layer of soft sand rock was made by compacting sand-clay-cement mixture layer by layer; meanwhile the target unit weight of each 30 mm layer of compacted mixture was confirmed. Immediately after casting the mixture, the model tubular piles were installed vertically into the unsolidified mixture with a pile guide to the specified depth, and fixed the pile position. The casted mixture was cured for 14 days in order to achieve the targeted strength (q_u) and stiffness of the embedded medium. The detailed preparation procedures and mechanical properties of the soft sand rock material are reported by Kunasegaram et al. (2015). It is important to note that sand and soft rock was filled inside the pile up to the ground surface level with the pile installation process employed in the model preparation process, which was confirmed by means of physical measurements.

After 14 days curing for the soft sand rock or upon the completion of sand model, the loading jack and laser displacement sensors (LDTs) were mounted on the container. Thereon the container moved to centrifuge platform and rigidly fixed, then the centrifugal acceleration was increased up to $50g$. One way horizontal load cycles were applied by the jack from small to large pile top displacements as described in **Fig. 3** at $50g$ environment. Applied horizontal load at the pile top (P_L) was measured by a load cell and horizontal displacement

(δ_t) and rotation (θ_t) at the pile top was obtained by means of LDTs at two elevations as described in **Fig. 1**. In Model 3, due to the less accurate measurements by LDTs, the pile top displacements were only measured by using the potentiometer attached to the loading jack as described in **Fig. 2**.

Having completed one loading test, the centrifuge was once stopped and the loaded pile was removed. Resetting the jack and LDTs to the next pile and the same horizontal loading was repeated. The loading was conducted in the sequence of Pile-S, Pile-M and Pile-L. In the loading of Pile MS_L of Model 1, due to the trouble of loading jack, unloading at the small displacements could not be made. While the pile SR_S of Model 3 was accidentally preloaded about 1 mm prior to the test without instrumentation, the stiffness and resistance could not be obtained in the intact condition for the small displacement range. In the following chapter, the test results are shown in prototype scales.

3. Results and discussion

3.1. Load-displacement and failure behaviour

A typical observed cyclic load (P_L) - displacement (δ_t) curve is presented in **Fig. 3**. In each cycle, certain amount of residual displacements can be seen after unloading. However, in the reloading processes the P_L - δ_t curves return to a unique curve, which is the envelope of cyclic load-displacement behaviour. Here onwards the envelope curve will be written as a backbone curve.

Fig. 4 shows the backbone curves obtained in the loading tests of all tested piles (**Table 1**). Observed structural failures of piles in different mediums are also

shown in **Fig. 5**. The influence of embedded medium and embedment depth under identical loading conditions can be clearly confirmed from **Fig. 4**. The deeper the embedment is, the larger the mobilized resistance of pile can be observed. However, this observation is not true while comparing the behaviour of piles DS_L and DS_M. There is no significant difference between the two piles, implying less effects of embedment depth increase from 9 m to 11.5 m in the dense sand. As shown in **Figs. 5(a), (b)** and **(c)**, structural failures of the pile were confirmed with clear local buckling point below the ground level for MS_L, DS_M, DS_L piles. Once the pile failed by the structural buckling, the further increase of embedment depth (d_e > 11.5 m for medium dense, d_e > 9m for dense sand) could have no significant influence on the lateral resistance of piles for abovementioned loading conditions. The reductions of resistance after the peak load are the indication of structural failure, while for MS_S, MS_M, and DS_S piles, the resistance increased until large pile top displacement over 50% of pile diameter (Φ) without showing peak resistance.

For the piles embedded in the soft sand rock, 1 m increment in embedment depth can significantly increase the ultimate lateral resistance up to d_e=4m. As a clear structural failure with local buckling was observed slightly above the ground level for SR_L pile with 4m embedment depth as shown in **Fig. 5(f)**, it can be inferred that further increase of the embedment could not contribute to the increase of pile lateral resistance.

The depth over which the effect of embedment increment cannot be obtained is considered as an “optimum embedment depth”. The difference of optimum embedment depth in the medium dense sand, dense sand, and soft rock can be attributed to their rigidity or confinement. The soft rock can effectively hold the pile at shallow depth even for the relatively stiff large diameter pile.

No structural failures were observed in SR_S and SR_M piles in the soft rock (**Fig. 5(e)**), but the load - displacement curves of the two piles also showed clear peak resistance and the reduction. The peak load displacement of SR_S was smaller than that of SR_M. These behavior of the piles with no pile failure but ground failure of the soft rock is different from that of the sand. This can be attributed to the strain softening of

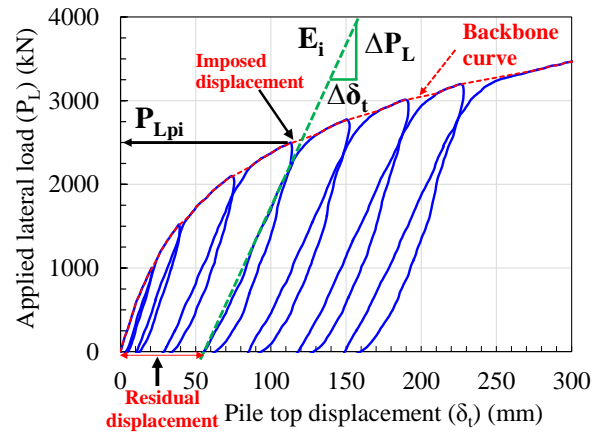


Fig. 3 Typical cyclic load-displacement behaviour

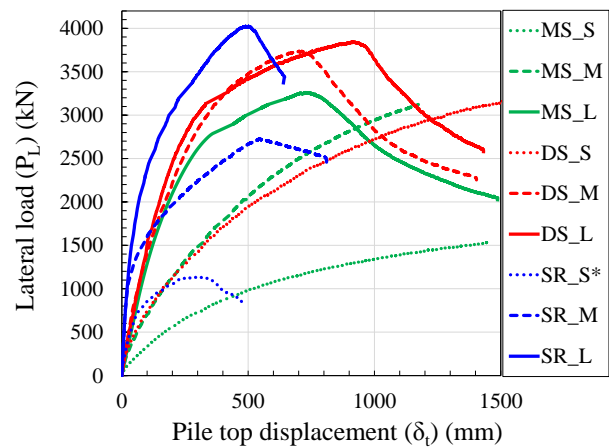


Fig. 4 Envelope curves observed from cyclic load-displacement behaviour (Back bone curves)

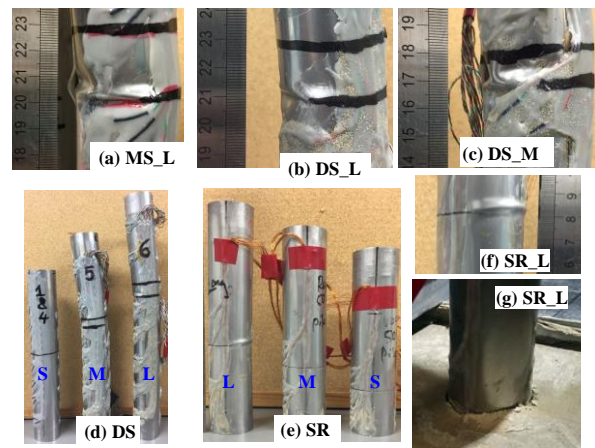


Fig. 5 Pile deformation and failures, and ground failure

stress-strain relationship of the rock material and smaller embedment depth of the soft rock model than that of sand model. Although the piles with structural failure and the piles embedded in the soft rock with relatively small d_e

showed strain softening behaviour in the load-displacement curves, the post peak resistance reduction are different between the piles failed by the structural failure and the ground failure. Once the structural buckling initiated a sudden reduction of load against the displacements can be seen. On the other hand, the observed post peak behaviour related to ground failures (SR_S*, SR_M) exhibited smaller post peak stiffness and much more ductile especially for the deeper embedment case (SR_M)).

3.2. Influence of embedment depth

The influence of embedment depth (d_e) on lateral resistance of piles embedded in different mediums from small to large pile top displacements (δ_t) are depicted in **Fig. 6**. It is important to note that the load corresponding to the pile top displacements of $50\% \Phi$ was considered as ultimate resistance (P_{ult}) for the piles without peak resistance in the load - displacement relation (**Fig. 4**). A distinctive behavior of piles at different displacement levels depending on the stiffness of embedded medium can be observed. In Model -1 (MS), as the embedment depth increases, the lateral resistance also increases from small to large displacements. However, the increment trends of resistance from $d_e = 6.5$ m to 9 m depth and $d_e = 9$ m to 11.5 m change with imposed displacement. At the small displacement ($\delta_t < 2\% \Phi$) the resistance increases linearly with d_e , while at $\delta_t = 4 \sim 10\% \Phi$, the larger resistance increase can be seen for the increment of d_e from 9 m to 11.5 m than that of 6.5 m to 9 m. However, the effect of former depth increment on P_{ult} become less than that of the latter increment. This is a clear evidence that the pile horizontal resistance or stiffness was mobilized by the soil in the early stage of loading but controlled by the strength and stiffness of pile at the ultimate conditions as discussed in **Fig. 4** and **Fig. 5(a)** for the pile (MS_L). In Model-2 (dense sand), the piles with $d_e = 9$ m and 11.5 m show almost no difference in the mobilized resistance from small displacement to ultimate values.

The horizontal resistance of piles embedded in the soft rock also increased with d_e . But the trend is quite different from that in sand. Large increase of lateral resistance can be attained by increasing d_e from 2 m to 4 m, almost linearly with d_e for all displacements, except the piles with d_e over 3 m at small displacements.

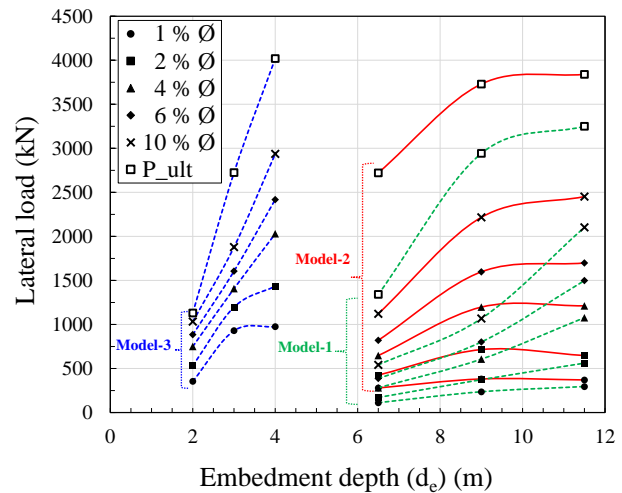


Fig. 6 Influence of embedment depth (d_e) on lateral resistance of piles embedded in sand and soft rock

The resistance of SR_L is almost the same and slightly larger than that of SR_M piles at $\delta_t = 1\% \Phi$ and $2\% \Phi$ respectively. At the small pile displacement the shallower depth of the rock (less than 3 m) could mainly confine the pile by the large stiffness of intact rock. But the softening of rock by the displacement deteriorates the subgrade reaction of shallow depth and cause the difference in resistance between SR_M and SR_L piles.

As overall behavior it can be concluded that the lateral resistance of pile embedded in sand and soft rock increases with increasing embedment depth if the ground stiffness dominates the resistance. However, the effect of the embedment depth over the optimum depth has no significant contribution.

3.3. Bending behaviour of pile

Measured bending moments along the pile at different pile top displacements (1%, 4%, 10% & 20% Φ) for sand and soft rock models are presented in **Fig. 7**. Depths at the maximum bending moment for the piles embedded in sand (MS, DS) are about -0.5 m for pile-S ($d_e = 6$ m), -2 m for pile-M ($d_e = 9$ m) and -2.5 m for pile-L ($d_e = 11.5$ m). The bending moments of the pile in the sand models increase almost linearly with the distance from the loading point to the depth of maximum bending moment. The observation clearly indicates that the confining stresses from shallow layers of the sands has less significant influence on the lateral resistance of piles. On the other hand, the piles in the soft rock showing the maximum moment was observed at slightly above

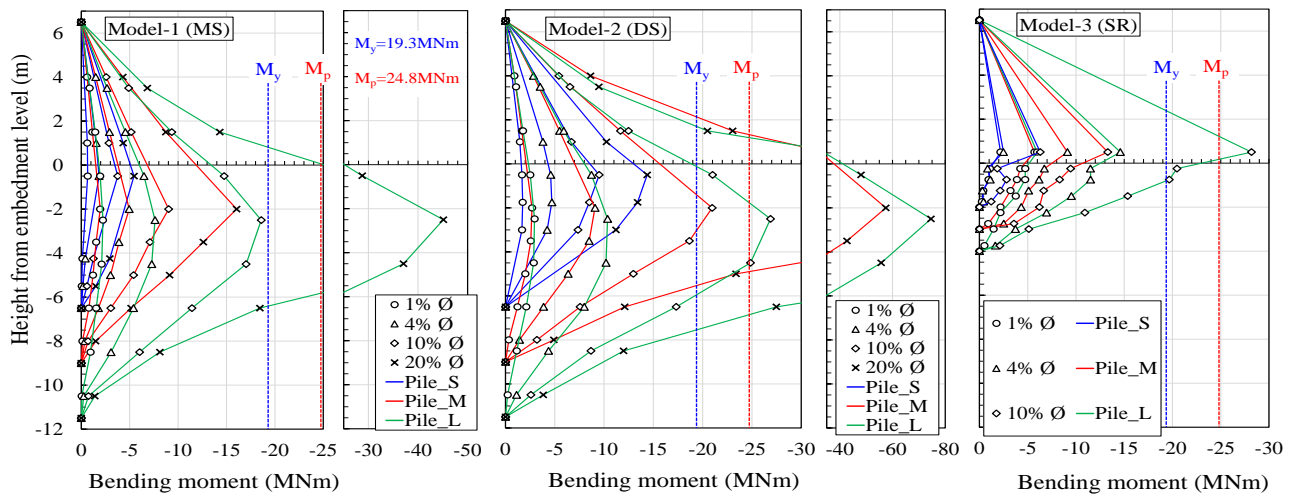


Fig. 7 Measured bending moment profiles at different pile top displacement

the ground surface. An abrupt change in the bending moments above and below the ground surface can be also observed. This observed bending behaviour is another evidence of very high confinement of shallow layers of soft rock.

The depths of local buckling were 1.5m in MS_L, 1.0m in DS_M&L, for the sand model and 0.15m above the ground surface for SR_L, which were shallower than the depth of maximum bending moment. This could indicate the effect of infilled materials in the pile up to the ground surface. Therefore, without this plugging effect, ultimate resistance of the structurally failed piles could have been smaller than the observed resistance.

Up to $\delta_t = 4\% \Phi$ (80 mm), all piles show the bending moment smaller than the yielding moment (M_y). At $\delta_t = 10\% \Phi$ (200 mm), MS_M and MS_L piles in the medium dense sand exhibit the bending moments slightly below and about the yielding moment respectively. However DS_M and DS_L piles in the dense sand with similar embedment depths reached the bending moments corresponding to yielding and plastic hinge (M_p) respectively at $\delta_t = 10\% \Phi$. At $\delta_t = 20\% \Phi$, piles MS_L, DS_M and DS_L had already reached the plastic limit, therefore this is a clear evidence for the structural deformation observed in **Fig. 5(a, b & c)**. The pile SR_L exhibits the bending moment higher than the plastic limit at a pile top displacement of $10\% \Phi$. As the stiffness of the ground increases from MS, DS to SR, the pile reaches its yielding and plastic limits at small displacement, which increases the possibility of structural failure over the soil failure in hard mediums.

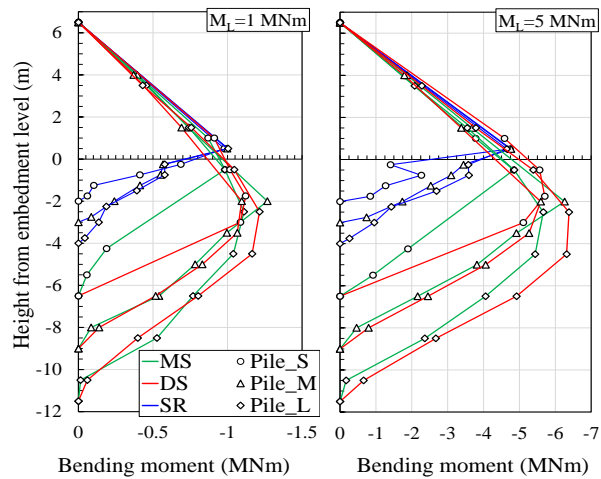


Fig. 8 Measured bending moment profiles at different

It can be also confirmed that the increasing embedment depth over the optimum depth in relatively hard embedment mediums cannot prevent the ultimate failure since it is caused by structural hinge. In other words, it can be said that the increasing section modulus can increase the optimum depth and the ultimate resistance.

Measured bending moment profiles observed at the moment load of 1 and 5 MNm. The moment load defined by horizontal load times the loading height at the ground surface is compared for all the piles in **Fig. 8**. Some strain gauges of the short piles in the two sand models did not work. Excluding the short piles, similar bending moment profiles were measured in the medium and long piles in the two sands respectively. The difference between the middle and long piles are more evident, i.e., the longer the piles are, the larger the moment in the deep portion becomes. This implies that as the load increases, the

resistance mobilization at the deep depth becomes larger relative to the shallower depth. While in the soft rock model, 3m and 4m embedded piles showed almost the same bending moment from the loading point up to -2m till the moment load of 5MNm and very small bending below this depth. Thanks to the large stiffness and strength of the intact rock, the observation implies that the large horizontal resistance concentrated at the very shallow depth against relatively small load.

3.4. Residual displacement

Fig. 9 illustrates the observed relationships between imposed and residual displacements (see **Fig. 3**). Despite the embedded medium, almost linearly increasing trend of residual displacements against the imposed displacements with different rates of increment can be observed. The larger the embedment depth is, the smaller the observed residual displacement under the same imposed displacements. From this result, it can be said that the long piles behave as flexible meanwhile the behaviour of short pile is rigid. In the initial stage of imposed displacements, almost zero residual displacements can be observed for the piles SR_M and SR_L, which could be attributed to the elastic recovery of the piles in soft rock. However, the piles in sand exhibits certain amount of residual displacements even at small imposed displacement, this phenomenon can be caused by local densification of soil behind the pile which could prevent the elastic recovery.

Large diameter piles are being used as mono-pile foundation for wind turbines, where one way cyclic loads by wind forces are the typical loading condition. Due to one-way cyclic loads, the accumulation of residual displacement and permanent movement of foundation and super structure could be a major concern for a long term stability of such large geotechnical structures.

In order to discuss the ground stiffness and the influence of embedment depth on the permanent deformation of mono-pile foundations, the relationship between residual displacement at the pile top and the normalized applied pre-maximum load in previous cycle (P_{Lpi} , see **Fig. 3**) by the ultimate load (P_{ult}) is presented in **Fig. 10**. P_{Lpi}/P_{ult} is a kind of load factor. As an overall trend, the residual displacements for the same load factor are reduced by increasing the ground stiffness from medium dense sand, dense sand to soft rock. From this trend, it can

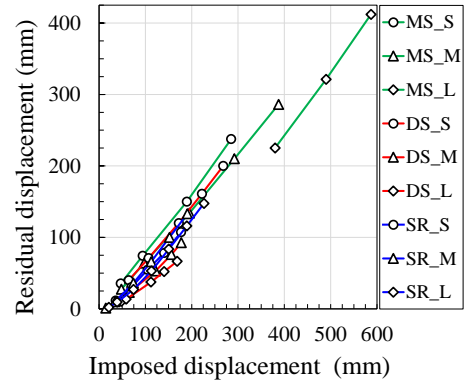


Fig. 9 Relationship between imposed and residual displacement

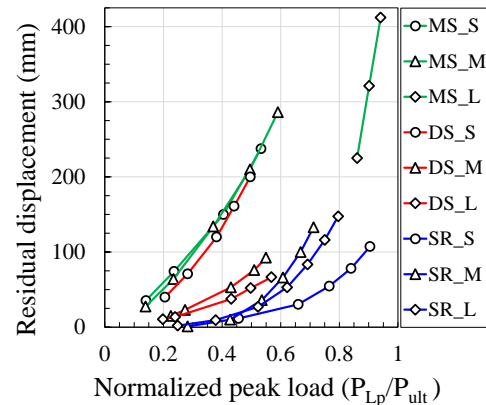


Fig. 10 Relationship between residual displacement and normalized load

be said that the displacement should be the dominant factor compared to the ultimate failure for the soft ground, while for the stiff embedment medium, securing the factor of safety against failure tends to be a critical condition in the foundation design.

3.5. System stiffness and residual displacements

Observed system stiffness (E_i) of each cycle is plotted against the applied pre-maximum load (P_{Lpi}) in the previous cycle in **Fig. 11**. It should be noted that in SR_S pile the observed stiffness was affected by the unintentional preloading, and in MS_L pile the stiffness under small load could not be measured, but only measured after the large loading history. Nonetheless, effects of embedment medium and depth can be clearly confirmed from the figure. The initial stiffness very much depends on the ground stiffness, much higher for the soft rock compared to sands, even though the embedment depth of the rock was about one third of that of the sand. However, the significant deterioration of the stiffness took place for the soft rock, but not in the sand. To scrutinize

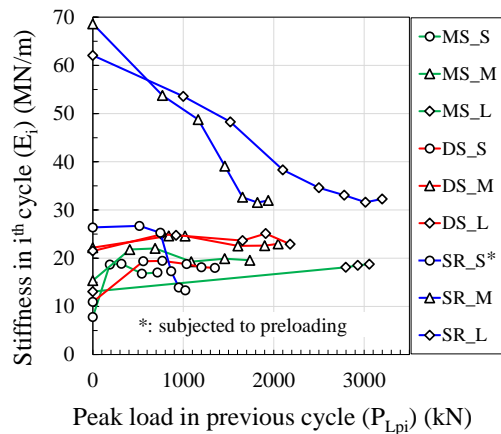


Fig. 11 Variation of stiffness in each cycle with applied peak load in previous cycle

the change of the system stiffness by the cyclic loading history, the normalized stiffness by initial one (E_i/E_0) is plotted against the normalized peak load (P_{Lpi}/P_{ult}) in **Fig. 12**. From this figure, the larger increase of the stiffness, in other words the effect of hardening can be seen for the medium dense sand than the dense sand, and also for the short pile than the long piles. While in the soft rock, the initial stiffness of middle ($d_e=3m$) pile and long piles ($d_e=4m$) are almost the same, but the stiffness deterioration was more significant for the middle pile than the long pile. However, the deteriorated stiffness at $P_{Lpi}/P_{ult}=0.5$ were about two times larger than that of increased stiffness of pile in the sands.

As discussed on the lateral resistance in **Fig. 6**, over a certain embedment depth, the effect of the depth becomes less significant, especially for ultimate resistance due to the pile structural failure and “optimum embedment depths” can be defined. However, the optimum embedment depth depends on the conditions of resistance, shallower for the initial stiffness than the ultimate bearing capacity in the soft rock.

4. Conclusions

From this study, the following conclusions were derived. In the stiff ground like the soft rock, the lateral resistance changes significantly in a small range of embedment depth. A small increment of embedment depth in soft sand rock highly controlled the displacement and failure behaviour of the piles compared to the increment in the sand soil. However, over some depth, the increment of pile length becomes less significant on the increase of resistance. This depth can be considered as an optimum

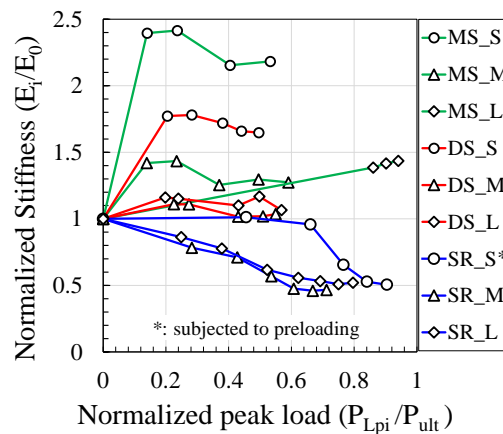


Fig. 12 Relationship between normalized stiffness and normalized peak load in previous cycle

depth. On the other hand, due to the softening of ground materials and the change of failure mode from the ground failure to pile structural failure, the optimum embedment depth changes depending on the conditions of resistance, shallower for the initial stiffness than the ultimate bearing capacity in the soft rock.

From the observations, it can be confirmed that the determination of the rational embedment depth considering given conditions is the most critical step in the design of this type of pile foundation.

5. Acknowledgements

The authors gratefully acknowledge the invaluable advice and guidance provided by the members and advisers of the IPA TC1 (Committee on Application of Self-retaining Tubular Pile Wall to Stiff Ground) in connection with the preparation of this paper.

References

- Association of Steel Pile. 2009. Design manual of self-standing steel sheet pile wall.
- Ishihama, Y., Fujiwara, K., Takemura, J. and Kunasegaram, V. 2018. Evaluation of deformation behavior of self-standing retaining wall using large diameter steel pipe piles into hard ground. Proc. 1st ICPE.
- Kunasegaram, V., Akazawa, S., Takemura, J., Seki, S., Fujiwara, K., Ishihama, Y., and Fujii, Y. 2015. Modeling of soft rock for a centrifuge study, Proc. 12th GeoKanto, pp. 15-19.
- Tatsuoka, F., Goto, S. and Sakamoto, M. 1986. Effects of some factors on strength and deformation characteristics of sand at low pressures. Soils and foundations, 26 (1), pp. 105-114.